NANO LETTERS

2008
Vol. 8, No. 10
3131-3136

Pulse-Loaded Ferroelectric Nanowire as an Alternating Current Source

Yue Zheng,† C. H. Woo,* and B. Wang‡

Department of Electronic and Information Engineering, The Hong Kong Polytechnic University, Hong Kong SAR, China

Received May 6, 2008; Revised Manuscript Received August 4, 2008

ABSTRACT

The behavior of an uniaxially pulse-loaded ferroelectric nanowire is simulated using a Landau−Ginzburg type thermodynamic model. Our results show that under a load of suitable magnitude and frequency, an appropriately dimensioned ferroelectric nanowire can produce a sizable alternating current voltage, sufficient for applications as a nanopower source for energy harvesting, or as an effective nanomechanical sensor.

Theories and experiments on ferroelectric thin film (TF), nanoparticles (NP), nanodisks (ND), nanobars (NB), nanorods (NR), nanowires (NW), and nanotubes (NT) indicate that their phase-transition or near-phase-transition properties, such as the Curie temperature, polarization, and susceptibility, are very sensitive to applied stresses. Thus, stresses produced by surface tension have been known to significantly affect the Curie temperature and other related properties.[1−6] Indeed, the transition temperature and Curie−Weiss relation of ferroelectric NT have also been found in our own work[7] to depend on stresses generated from effects such as surface tension and surface effect, resulting in remnant polarization and coercive fields that may exceed the bulk values.

Although a quantitative and detailed investigation of the effects of mechanical loads on the physical properties of a ferroelectric NW has yet to be performed, the general dependence of the para/ferroelectric transition on an applied load has led several authors to experiment with the idea of alternating current (ac) generation using a pulsed mechanical load. Indeed, Wang et al.[8−10] demonstrated the feasibility of dc generation based on the conversion of mechanical loading in the form of bending of single piezoelectric NWs, such as ZnO and GaN NWs, using the tip of a conductive atomic force microscope (AFM). Yu et al.[11,12] succeeded in generating periodic charge and ac voltage from a single-crystal $BaTiO_3$ NW subjected to a pulsed tensile load, suggesting the feasibility of using such perovskite piezoelectric nanowires for efficient energy-harvesting applications.

In the present work, we consider the combined effects of sample dimension, surface tension and pulsed mechanical loads on the properties of a ferroelectric NW. A thermodynamic model based on the Landau−Ginzburg free-energy functional is used, in which work due to the mechanical and electrical loading, both internal and external, are taken into account. The dynamic behavior of the sample is simulated by solving the associated Euler−Lagrange equation as a function of time. The transition temperature, polarization, and the ac current generated are calculated as a function of the sample dimensions and mechanical load. The efficiency and usefulness of ferroelectric NWs as an ac voltage generator is evaluated.

Formulation. ***The System Free Energy.*** We use as thermodynamic reference a ferroelectric crystal in which there are no applied fields,[7,13−17] that is, electric, magnetic, and mechanical (internal or external). Let $\boldsymbol{P}$ be the spontaneous polarization of the reference crystal. The application of an electric field $\boldsymbol{E}$ (including the external electric field $\boldsymbol{E}_{\mathbf{ext}}$ and the depolarization field $\boldsymbol{E}_{\mathbf{d}}$) also induces a polarization $\boldsymbol{P}^{\mathrm{E}}$. To the lowest order, $\boldsymbol{P}^{\mathrm{E}}$ is linearly proportional to $\boldsymbol{E}$ and can be written as $\boldsymbol{P}^{\mathrm{E}} = \chi_{\mathrm{b}}\boldsymbol{E}$, with background susceptibility χ_{b}, which is characteristic of the background materials far from the phase transition in paraelectric state. The total polarization $\boldsymbol{P}^{\mathrm{T}}$ is therefore a sum of $\boldsymbol{P}$ and $\boldsymbol{P}^{\mathrm{E}}$. The electric displacement is then[15−17]

$$\boldsymbol{D} = \varepsilon_0\boldsymbol{E} + \boldsymbol{P}^{\mathrm{T}} = \varepsilon_0\boldsymbol{E} + \chi_{\mathrm{b}}\boldsymbol{E} + \boldsymbol{P} = \varepsilon_{\mathrm{b}}\boldsymbol{E} + \boldsymbol{P} \quad (1)$$

where ε_0 are dielectric constants of the vacuum. $\varepsilon_{\mathrm{b}} = \varepsilon_0 + \chi_{\mathrm{b}}$ is the dielectric constant of the background material. When surfaces are introduced, effects of the depolarization field have to be added. Indeed, in the absence of an external electric field, the total electric field has only one contribution that is the depolarization field $\boldsymbol{E}_{\mathbf{d}}$, that is, $\boldsymbol{E} = \boldsymbol{E}_{\mathbf{d}}$, the electric displacement is given by[15−17]

* To whom correspondence should be addressed. E-mail: chung.woo@polyu.edu.hk.
† From Electro-Optics Technology Center, Harbin Institute of Technology, Harbin, China.
‡ Permanent address: School of Physics and Engineering, Sun Yat-sen University, Guangzhou, China.

10.1021/nl801294n CCC: $40.75
Published on Web 09/10/2008

$$\boldsymbol{D} = \varepsilon_0 \boldsymbol{E}_{\mathbf{d}} + \boldsymbol{P}^{\mathrm{T}} = \varepsilon_0 \boldsymbol{E}_{\mathbf{d}} + \chi_{\mathrm{b}} \boldsymbol{E}_{\mathbf{d}} + \boldsymbol{P} = \boldsymbol{\varepsilon}_{\mathbf{b}} \boldsymbol{E}_{\mathbf{d}} + \boldsymbol{P} \qquad (2)$$

According to Landau−Lifshitz,[16] the free-energy can be expressed as a functional of the functions $\boldsymbol{P}$ and $\boldsymbol{E}$, given by $G(\boldsymbol{P},\boldsymbol{E}) = G(\boldsymbol{P},\boldsymbol{E})|_{E=0} - \int_0^E \boldsymbol{D}\cdot \mathrm{d}\boldsymbol{E}$. Here we note that $G(\boldsymbol{P},\boldsymbol{E})|_{E=0}$ is the free-energy functional of the field-free, uniform, and infinite (surfaceless) crystal that we use as reference. We note that expressed this way, quasi-equilibrium evolution of the system away from the reference state due to the application of the electric field $\boldsymbol{E}$ is governed by the dynamic equation $\partial G/\partial \boldsymbol{E} = -\boldsymbol{D}$.

In this work, we consider a ferroelectric nanowire (FNW) sandwiched between metal electrodes as shown in Figure 1. The FNW is assumed to be a perfect insulator with short-circuited electrodes, with length and radius denoted by h and R, respectively. To simplify the formulation and computation, axial symmetry is assumed, so that all vector fields in the NW are directed in the z-direction, and all the foregoing vectors can be represented only in terms of their magnitudes. In this regard, we note that the directions of the polarization are not necessarily all along the z-direction, and radial components should be considered in general. Nevertheless, under short-circuit electric condition, the radial compression due to the surface tension, and the uniaxial loading along the z-direction, the polarization is most easily aligned along the z-direction.

Under short circuit boundary conditions, the depolarization field can be estimated by $E_{\mathrm{FE}} \approx -\eta(R,h)[P(z,r) - q_{\mathrm{e}}]/\varepsilon_{\mathrm{b}}$, where q_{e} is the compensation charge density at the top and bottom electrodes, which can be expressed as $q_{\mathrm{e}} = \langle P \rangle = 1/V \iiint_V P\,\mathrm{d}v$ under conditions of electrostatic equilibrium, where V is the volume of FNW. $\eta(R,h)$ can be estimated using the relation $\eta(R,L) \approx 1/[1 + (h/2R)^2]$.[4] In the present work, we only consider cases where the ratio $h/2R \geq 10$. The corresponding value of $\eta(R,h)$ is less than 1%, thus justifying the neglect of the depolarization field E_{FE} in the present paper.

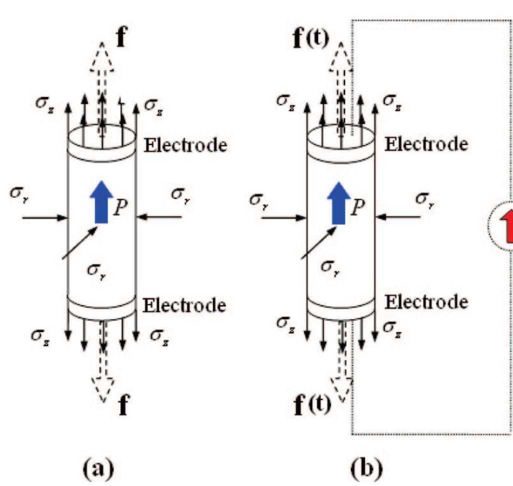

Figure 1. Schematics of a ferroelectric NW under the effective radial pressures and external mechanical stress load with (a) open-circuit boundary condition, (b) short-circuit boundary condition.

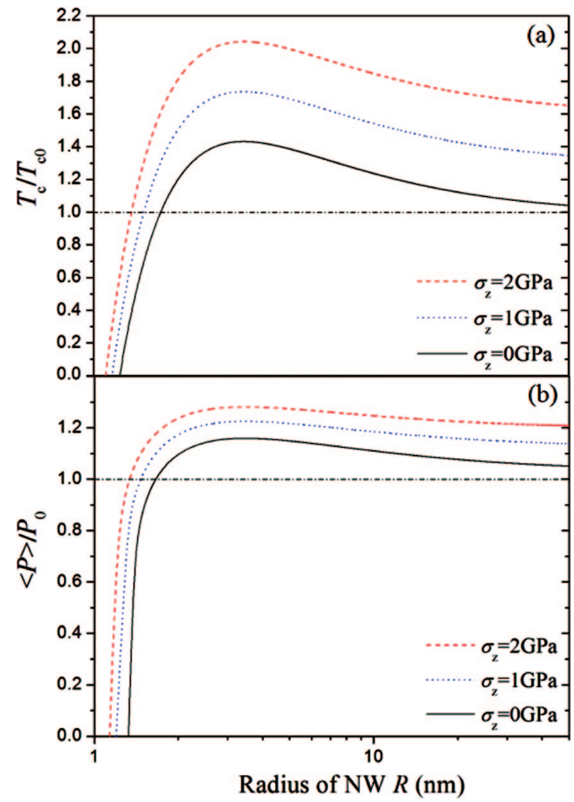

Figure 2. (a) The normalized T_c/T_{c0}, and (b) P/P_0 at room temperature of NW with different tensile stress loads.

Taking into account the surface tension and the uniform external applied stress σ_z, the total free energy F of the FNW can be written with the field-free infinite crystal as a reference state as[4,13,17]

$$F = 2\pi \int_{-h/2}^{h/2} \mathrm{d}z \int_0^R r\mathrm{d}r \Big\{ \Big[\frac{\alpha}{2} - 2Q_{12}\sigma_s(\mu,R) - Q_{11}\sigma_z \Big] P^2(r,z) + \frac{\beta}{4}P^4(r,z) + \frac{\gamma}{6}P^6(r,z) + \frac{g}{2}[\nabla P(r,z)]^2 - (s_{11}+s_{12})\sigma_s^2(\mu,R) - \frac{1}{2}s_{11}\sigma_z^2 - 2s_{12}\sigma_s(\mu,R)\sigma_z \Big\} + F_s, \quad (3)$$

where α, β, and γ are the free-energy expansion coefficients of the corresponding bulk material, with $\alpha = \alpha_0(T - T_{c0})$, and α_0 being proportional to the inverse Curie constant. T_{c0} is the Curie temperature of the reference bulk crystal (field-free and surfaceless). g is the gradient coefficients base on Landau−Ginzburg theory.[18−20] Q_{11} and Q_{12} are the components of the electrostrictive tensor. s_{11} and s_{12} are components of the elastic compliance tensor. $\sigma_s(\mu,R)$ is the uniform compressive radial stress induce by the surface tension, given by $\sigma_s(\mu,R) = -\mu/R$.[1,2,4,5,7,21] μ is the effective surface tension coefficient. σ_z is the external applying stress along the z-direction determined by the external applying force f, and $\sigma_z = f/(\pi R^2)$. F_s is the energy associated with the near-surface depolarization that include the planar end surfaces and the cylindrical sidewall.[22,23] Following refs 4 and 7, we assume that F_s can be empirically represented via the corresponding extrapolation lengths $\delta_{\text{u-p}}$ and $\delta_{\text{s-w}}$, and expressed in the following form:

$$F_s = g\int_0^R \frac{2\pi r}{\delta_{\text{u-p}}} dr[P^2(r, z = h/2) + P^2(r, z = -h/2)] + g\int_{-h/2}^{h/2} \frac{2\pi R}{\delta_{\text{s-w}}} dz P^2(r = R, z) \quad (4)$$

Effect of Mechanical Load. In variation of the free energy eq 3 with respect to P yields the Euler−Lagrange equations, the time evolution of the system is governed by the time-dependent Landau−Ginzburg (TDLG) equation,[3,13,14] which can be written as

$$\frac{\partial P(t,z,r)}{\partial t} = -M\frac{\delta F}{\delta P(t,z,r)}$$

$$= -M\left\{\alpha^* P(t,z,r) + \beta P^3(t,z,r) + \gamma P^5(t,z,r) - g\left[\frac{\partial^2 P(t,z,r)}{\partial z^2} + \frac{1}{r}\frac{\partial}{\partial r}\left(r\frac{\partial}{\partial r}P(t,z,r)\right)\right]\right\} \quad (5)$$

where $\alpha^* = [\alpha_0(T - T_{c0}) + 4Q_{12}(\mu/R) - 2Q_{11}\sigma_z]$, and M is the viscosity coefficient that causes the delay in motion of dipole moments. $\delta F/\delta P$ is the thermodynamic driving force responsible for the spatial and temporal evolution. The surface term in eq 3 yields the boundary conditions[4,7,13,18,19,24,25]

$$\frac{\partial P(t,z,r)}{\partial r} = -\frac{P(t,z,r)}{\delta_{s-w}}, \quad \text{for } r = R, \quad \text{and}$$
$$\frac{\partial P(t,z,r)}{\partial z} = \mp\frac{P(t,z,r)}{\delta_{\text{u-p}}}, \quad \text{for } z = \pm\frac{h}{2}, \quad (6)$$

Analytic expressions have been derived for the Curie temperature and critical thickness of ferroelectric TF and NT using the TDLG.[7,13] Results show that the phase transition temperatures are insensitive to the film thickness, tube radius and surface conditions. Analytically solving the nonlinear thermodynamic eqs 5 and 6 to obtain the evolution of the polarization field in the FNW is a cumbersome exercise. In this paper, we adopt the more convenient numerical approach instead, a finite difference method for spatial derivatives and the Runge−Kutta method for temporal derivatives are employed.[18,19,24−26]

The study in this paper is conducted for a $PbTiO_3$ NW, which has been successfully fabricated and implemented recently. Since typical values of the effective surface tension coefficient vary between 5 to 50 N/m,[1,4,7,18] we only use a value of $\mu = 15$ N/m. Other material constants, such as the electrostrictive and elastic coefficients,[27] the gradient coefficients,[18−20] the extrapolation lengthes,[3] are well known and listed in SI units as the following: $\alpha = 7.6 \times 10^5 (T - T_{c0})$, $T_{c0} = 752$, $\beta = -2.29 \times 10^8$, $\gamma = 1.56 \times 10^9$, $g = 3.46 \times 10^{-10}$, $Q_{11} = 0.089$, $Q_{12} = -0.024$, $s_{11} = 8 \times 10^{-12}$, $s_{12} = -2.5 \times 10^{-12}$, $\delta_{\text{s-w}} = \delta_{\text{u-p}} \approx 3 \times 10^{-9}$, $t_M = tM \times 10^{-3}$, $h/2R = 10$.

We first start with an infinitesimally positive polarized region at a random location at a constant temperature near phase transition. In the ferroelectric region, the initial perturbation will spread and grow into a stable polarization configuration. On the other hand, in the paraelectric region the initial polarized region will shrink away. Using this method, one can determine the relation between the phase transition temperature and the radius of the FNW. The phase transition temperature[7,13] T_c as a function of the radius R for different external applied stresses σ_z is as shown in Figure 2a. In the absence of the external load, that is, $\sigma_z = 0$ GPa, the effect of the surface tension can be immediately discerned from the peak of the transition temperature $T_c^{\max} \approx 1.4T_{c0}$ at $R \approx 3$ nm. For comparison, the calculation is repeated for external applied uniaxial tensile stresses of 1 and 2 GPa. It can be seen that in the present case an applied tension always raises T_c. For example, the maximum of phase transition temperature can more than double, reaching $T_c^{\max} \approx 2T_{c0}$ at $\sigma_z = 2$ GPa. As the compression due to the surface tension and external tensile stress stop to increase beyond the yield point, the surface effect described by the extrapolation length starts to dominate and lower the transition temperature as R decreases further. As a result, T_c shows a maximum of $T_c^{\max} \approx 2T_{c0}$ at a radius of $R \approx 3$ nm. From Figure 2a, the critical radius of the NW at which T_c vanishes, that is, ferroelectricity disappears permanently, can also be obtained. Similar observations for the existence of the critical ferroelectric size in NWs and thin films have been discussed in refs 4, 5, 7, and 13. Interestingly, besides increasing the transition temperature, the application of an external tensile stress also affects the polarization in the NW significantly. By solving eq 5, we obtain the average polarization of a PTO NW at room temperature as a function of radius R, which we plot in Figure 2b for different applied stresses, where P_0 is the spontaneous polarization of the reference bulk in which there is no applied fields. The similarity between Figure 2, panels a and b, is clear. Figure 2b also demonstrates the existence of a critical radius R_c of about 1.2 nm, below which the polarization disappears.

AC Generation under a Pulsed Load. We now investigate the response of a single FNW to an alternating tensile and compressive load, as shown Figure 1. Two time-dependent loading patterns are considered

(a)

$$\sigma_z(t) = \sigma^{\Delta}(t) = \begin{cases} \sigma_0 \dfrac{2(t - nT^{\Delta})}{T^{\Delta}}, & nT < t \leq (n + 1/2)T \\ \sigma_0 \dfrac{2[(n+1)T^{\Delta} - t]}{T^{\Delta}}, & (n + 1/2)T < t \leq (n + 1)T \end{cases} \quad (7a)$$

and

(b)

$$\sigma_z(t) = \sigma^{\frown}(t) = \sigma_0\left|\sin\left(\frac{2\pi t}{T^{\frown}}\right)\right| \quad (7b)$$

Here σ_0 and $T^{\frown} = 2T^{\Delta}$ are the amplitude and period of the external applied stress, respectively. Naturally, the corresponding applied force is given by $f_z(t) = \pi R^2\sigma_z(t)$. The evolution of the polarization P can then be calculated by solving the corresponding TDLG eq 5. Under an external axial load (see Figure 1) the average charge density in the electrodes q_e is governed by $\langle P\rangle$ as a function of the surface tension and external mechanical load. The current I can be described according to $I = dQ_e/dt = \pi R^2 dq_e/dt$, where Q_e is

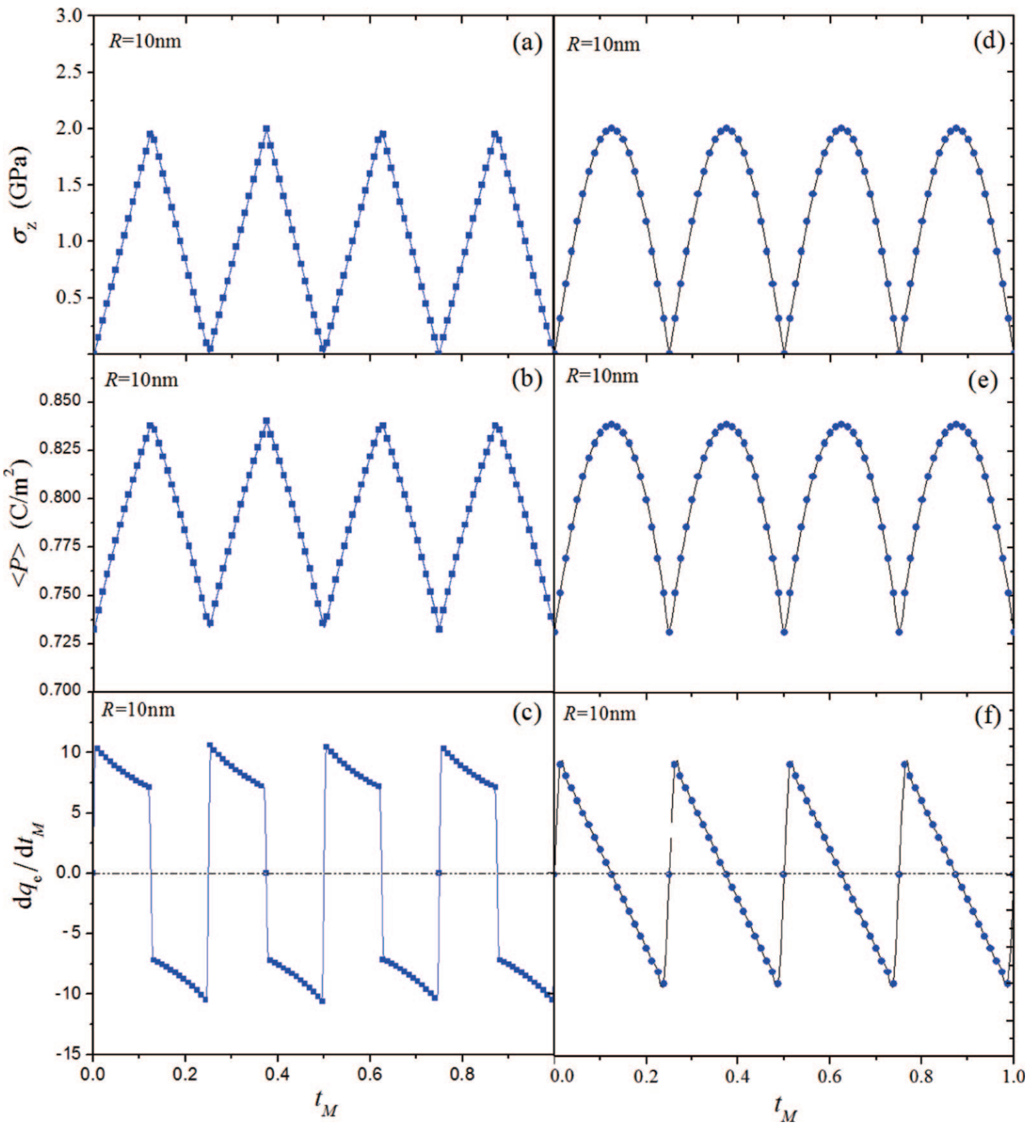

Figure 3. Under (a) a tensile stress load as $\sigma_z = \sigma^{\Delta}$, (b) response of the average polarization, (c) the current density of NW system with short-circuit condition. Under (d) a tensile stress load as $\sigma_z = \sigma^{\cap}$, (e) response of average polarization, (f) the current density of NW system at room temperature.

the total charge in the electrodes. Here dq_e/dt is the current density.

It is expected that the voltage across the electrodes will change in response to the change of the polarization field in a short-circuited NW, when the transition temperature changes. This voltage is transient in nature and drives an electric current across the electrodes, which lasts only until the polarization charge in the NW, or the lack of it, is completely balanced by the free charges driven across.

In general, one must consider in detail the effects of the time lag between the relaxation of the polarization field and that of the compensating free charges.[28−30] We note that the kinetic coefficient M should vary with the size of the NW and the temperature. When the FNW is in the ferroelectric state away from the phase transition point, M is large. On the other hand, when the FNW is close by the transition point, the value of M would drastically reduce. In the present study, we assume the former case and use the generalized time as $t_M = tM$ as in many other works for investigating kinetic properties of ferroelectrics based on TDLG and Landau−Khalatnikov (LK) equations.[13,18,19,24−26] In our calculation, we neglect for simplicity the transient assuming it is short compared to the cycle time of the mechanical load. Under this assumption, the time lag between the mechanical load and the response of the polarization charge compensation may be neglected if the frequency of mechanical load is not excessively high.

As described in the previous section, the steady polarization P can be obtained numerically from the TDGL of eq 5. Figure 3 shows the responses of $\langle P \rangle$ (Figure 3b, e) and current density (Figure 3c,f) of the NW system to the cyclic mechanical loads (Figure 3a, d). Here the external mechanical force f_z is only from 0 to 0.628 μN. The response can be seen to be highly sensitive to external mechanical force. An ac with current density can be generated using a periodic tensile load on the order of micro-Newtons. Figures 4 shows the effect of the magnitude of the mechanical load on the polarization and current of PTO NW. Figure 5 show the

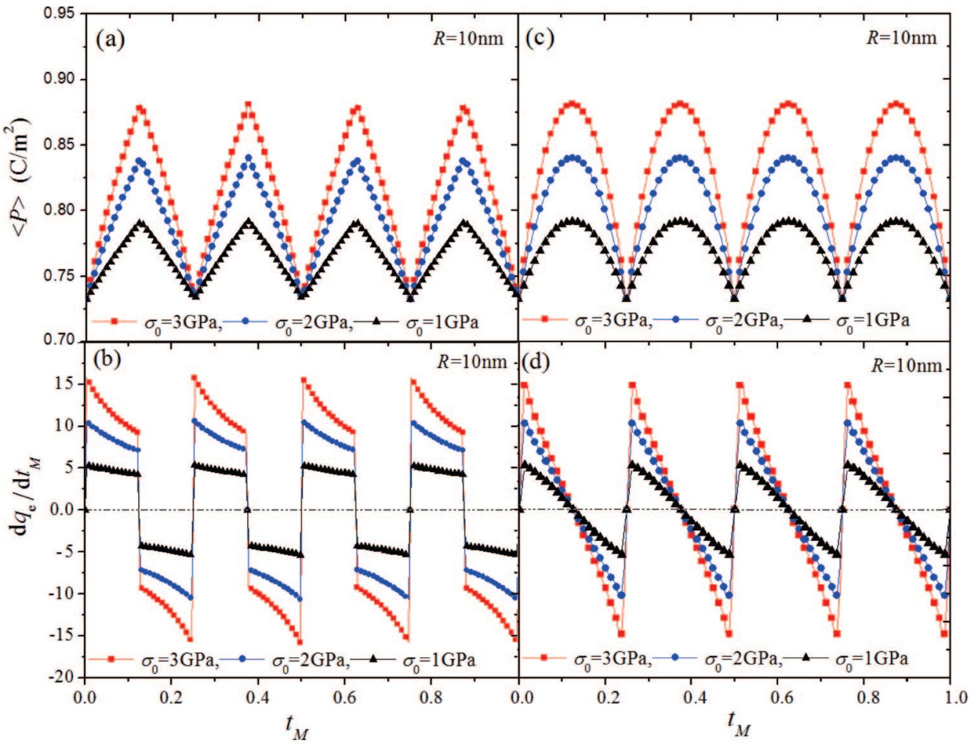

Figure 4. Under different tensile stress loads as type of $\sigma_z = \sigma^{\Delta}$, (a) response of average polarization, (b) the current density of NW system. Under different tensile stress loads as type of $\sigma_z = \sigma^{\cap}$, (c) response of average polarization, (d) the current density of NW system, at room temperature.

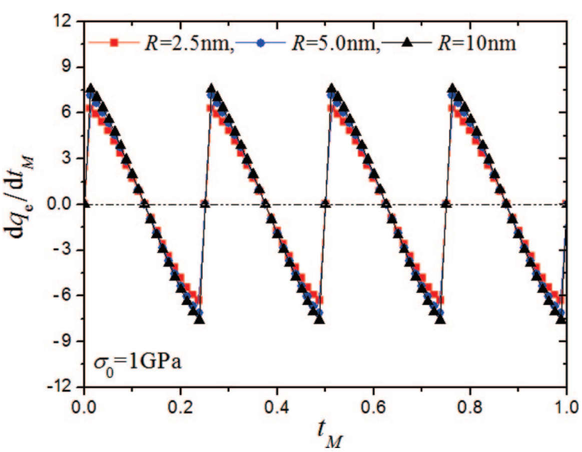

Figure 5. Under a tensile stress load as type of $\sigma_z = \sigma^{\cap}$ the current density of NW system with different NW's sizes at room temperature.

dependence on the dimensions of the FNW. They are all significant.

We note that in the foregoing we only consider the operation mode in which the FNW is always in the ferroelectric state. One may also consider another operation mode of higher efficiency and sensitivity in which the system is driven across the phase transition, in which case the calculation would be more complicated, and the time lag between the driving mechanical load and the generated ac-voltage has to be considered more carefully.

In summery, using a thermodynamic model, the transition temperature, polarization of a ferroelectric nanowire near the para/ferroelectric transition is calculated numerically as functions of the applied mechanical load and the sample dimensions. Using the same methodology, the possibility of generating a useful alternating current from a single ferroelectric nanowire by applying a cyclic mechanical load is also investigated. The mechanically induced electric current is found to depend on the applied force and the dimension of the nanowire. These results show that ferroelectric NWs (or NRs and NBs) have sufficient strength to be potentially useful in applications such as a nanoscale ac generator for energy harvesting and as mechanical sensors of ultrahigh sensitivity.

Acknowledgment. This project was supported by grants from the Research Grants Council of the Hong Kong Special Administrative Region (G-YX0T, 5322/04E). Y.Z. is also grateful for support from the National Science Foundation of China (No. 10732100).

References

(1) Uchino, K. J.; Sadanaga, E. J.; Hirose, T. *J. Am. Ceram. Soc.* **1989**, *72*, 1555–1558.
(2) Zhou, Z. H.; Gao, X. S.; Wang, J.; Fujihara, K.; Ramakrishna, S.; Nagarajan, V. *Appl. Phys. Lett.* **2007**, *90*, 052902.
(3) Zhong, W. L.; Wang, Y. G.; Zhang, P. L.; Qu, B. D. *Phys. Rev. B.* **1994**, *50*, 698–703.
(4) Morozovska, A. N.; Eliseev, E. A.; Glinchuk, M. D. *Phys. Rev. B.* **2006**, *73*, 214106.
(5) Morozovskaya, A. N.; Eliseev, E. A.; Glinchuk, M. D. *Phys. B.* **2006**, *322*, 356–370, 2006.
(6) Naumov, I. I.; Fu, H. X. *Phys. Rev. Lett.* **2005**, *95*, 247602.
(7) Zheng, Y.; Woo, C. H.; Wang, B. *J. Phys.: Condens. Matter.* **2008**, *20*, 135216.
(8) Gao, Y. F.; Wang, Z. L. *Nano Lett.* **2007**, *7*, 2499–2505.
(9) Wang, Z. L.; Song, J. H. *Science* **2006**, *312*, 242–246.
(10) Wang, X. D.; Song, J. H.; Liu, J.; Wang, Z. L. *Science* **2007**, *316*, 102–105.
(11) Wang, Z. Y.; Hu, J.; Suryavanshi, A. P.; Yum, K.; Yu, M. F. *Nano. Lett.* **2007**, *7*, 2966–2969.

(12) Wang, Z. Y.; Hu, J.; Yu, M. F. *Nanotech* **2007**, *18*, 235203.
(13) Wang, B.; Woo, C. H. *J. Appl. Phys.* **2005**, *97*, 084109.
(14) Wang, B.; Woo, C. H. *J. Appl. Phys.* **2006**, *100*, 044114.
(15) Lines, M. E.; Glass, A. M. *Principles and Applications of Ferroelectrics and Related Materials*; Clarendon Press: Oxford, 1977.
(16) Landau, L. D.; Lifshitz, E. M. *Electrodynamics of continuous media*; Oxford University Press: New York, 1960.
(17) Woo, C. H.; Zheng, Y. *Appl. Phys. A* **2008**, *91*, 59–63.
(18) Wang, J.; Zhang, T. Y. *Acta. Mater.* **2007**, *55*, 2465–2477.
(19) Hong, L.; Soh, A. K.; Song, S. Y. C.; Song; Lim, L. C. *Acta. Mater.* **2008**, *56*, 2966–2974.
(20) Li, Y. L.; Hu, S. Y.; Liu, Z. K.; Chen, L. Q. *Acta. Mater.* **2002**, 395–411.
(21) Ma, W. H.; Zhang, M. S.; Lu, Z. H. *Phys. Status Solidi B* **1998**, *166*, 811.
(22) Zheng, Y.; Wang, B.; Woo, C. H. *Appl. Phys. Lett.* **2006**, *88*, 092903.
(23) Zheng, Y.; Wang, B.; Woo, C. H. *Appl. Phys. Lett.* **2006**, *89*, 062904.
(24) Blinc, R.; Zeks, B. *Soft Modes in Ferroelectrics and Antiferroelectrics*; North-Holland: Amsterdam, 1974.
(25) Wang, J.; Zhang, T. Y. *Acta Mater.* **2006**, *55*, 2465.
(26) Zheng, Y.; Wang, B.; Woo, C. H. *Acta Mater.* **2008**, *56*, 479–488.
(27) Pertsev, N. A.; Zembilgotov, A. G.; Tagantsev, A. K. *Phys. Rev. Lett.* **1998**, *80*, 1988.
(28) Li, S.; Eastman, J. A.; Vetrone, J. M.; Foster, C. H.; Newnham, R. E.; Cross, L. E. *Jpn. J. Appl. Phys.* **1997**, *36*, 5169.
(29) Strukov, B. A.; Levanyuk, A. P. *Ferroelectric Phenomena in Crystals*; Springer: New York, 1998.
(30) Tagantsev, A. K.; Sherman, V. O.; Astafiev, K. F.; Venkatesh, J.; Setter, N. *J. Electroceram.* **2003**, *11*, 5.

NL801294N